J. MATER. CHEM., 1991, 1(5), 843–855

Synthesis and Phase Behaviour of Mesomorphic Transition-metal Complexes of Alkoxydithiobenzoates

Crystal and Molecular Structure of Three Metal Alkoxydithiobenzoates

Harry Adams,[a] Ana Carmen Albeniz,[b] Neil A. Bailey,[a] Duncan W. Bruce,*[a] Ashvin S. Cherodian,[c] Rupinder Dhillon,[a] David A. Dunmur,[a] Pablo Espinet,[b] José L. Feijoo,[d]† Elena Lalinde,[a] Peter M. Maitlis,[a] Robert M. Richardson[c] and Goran Ungar[d]‡

[a] *Department of Chemistry, The University, Sheffield S3 7HF, UK*
[b] *Departamento de Quimica Inorganica, Universidad de Valladolid, Valladolid, Spain*
[c] *School of Chemistry, University of Bristol, Cantock's Close, Bristol BS8 1TS, UK*
[d] *Department of Physics, University of Bristol, Tyndal Avenue, Bristol BS8 1TL, UK*

Reaction of 4-alkoxydithiobenzoates (*n*-odtb, where *n* refers to the number of carbon atoms in the alkoxy chain) with divalent salts of nickel, palladium and zinc leads to complexes of the formula $[M(n\text{-odtb})_2]$ where M = Ni, Pd and $[Zn_2(n\text{-odtb})_4]$ which are mesomorphic. The shortest-chain homologues of the Ni and Pd complexes show a nematic phase while at longer chain lengths, an S_C phase is observed. Most homologues of the zinc complexes show a nematic phase with an S_C phase appearing only for the longest homologues. The gold(III) complexes $[AuX_2(n\text{-odtb})]$ are also mesomorphic and show the S_A phase. Single-crystal X-ray structure determinations have been carried out for $[Pd(8\text{-odtb})_2]$, $[Zn_2(4\text{-odtb})_4]$ and $[Zn_2(8\text{-odtb})_4]$, showing the first to be planar and the last two dinuclear with pseudo five-co-ordinate zinc atoms.

Keywords: *Liquid crystal*; *Crystal structure*; *Alkoxydithiobenzoate*; *Metallomesogen*

Currently, there is much interest in the synthesis and characterisation of liquid-crystalline materials containing metal atoms because of the potential to modify many physical properties *via* the inclusion of a metal centre. For example, high birefringence materials containing palladium,[2] paramagnetic species containing either copper[3] or vanadium[4] and iridium complexes with high electronic polarisabilities[5] have all been reported.

Another property offered by metal complexes is that of colour; highly coloured complexes which may be soluble in conventional calamitic materials could be useful as dyes in guest–host devices. The mesogenic dithiolenes reported by Giroud *et al.*[6] and some related species have been investigated as solutes in nematic hosts.[7]

We now report the synthesis, phase characterisation and X-ray studies of four series of metal complexes formed by binding 4-alkoxydithiobenzoate ligands to Ni^{II}, Pd^{II}, Zn^{II} and Au^{III}. Preliminary data from these studies have been published[8] and Ohta *et al.*[9] have recently reported the mesomorphism of one of the complexes described here. The Ni, Pd and Zn complexes described are all highly coloured and linear dichroism studies of these materials are reported in the following paper.

Results and Discussion

Ligand Synthesis

The 4-alkoxydithiobenzoate ligands were synthesised according to literature procedures[10] as shown in Scheme 1. Because of the relatively low stability of the free acids, the ligands were isolated and stored as their sodium salts.

Unlike the isostructural 4-alkoxybenzoic acids,[11] which are known to show nematic and smectic phases, the dithiobenzoic acids themselves did not show any mesomorphic behaviour. The mesomorphism in the benzoic acids results from the association of two molecules to form hydrogen-bonded dimers (see Fig. 1). That the dithiobenzoic acids are non-mesomorphic probably results from very much weaker intermolecular hydrogen bonds, which preclude the formation of dimers of sufficient stability. This is supported by molecular-weight measurements made on H8-odtb (4-octyloxydithiobenzoic acid) in toluene and chloroform which showed the acid to be essentially unassociated [calculated 282 g mol^{-1}; found 357 g mol^{-1} (toluene), 315 g mol^{-1} ($CHCl_3$)] in contrast to the alkyloxybenzoic acids which are clearly dimeric [nonyloxybenzoic acid, calculated (for the dimer) 528 g mol^{-1}; found 529 g mol^{-1} ($CHCl_3$)].

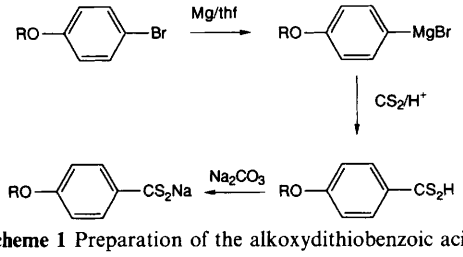

Scheme 1 Preparation of the alkoxydithiobenzoic acids

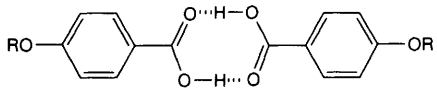

Fig. 1 Dimeric arrangement of benzoic acid derivatives

Synthesis of Metal Complexes

Gold

The yellow–orange gold complexes $[AuX_2(n\text{-odtb})]$ where X = Cl, Br, were prepared by reaction of [AuCl(tht)] where tht = tetrahydrothiophene, with the sodium salt of the acid to give the dimeric $[\{(n\text{-odtb})Au\}_2]$ which were then oxidised

† Present address: Departmento de Ciencia de Los Materiales, Universidad Simón Bolivar, Apolo 89000, Caracas 1080, Venezuela.
‡ Present address: School of Materials, University of Sheffield, Elmfield, Northumberland Road, Sheffield S10 2TZ, UK.

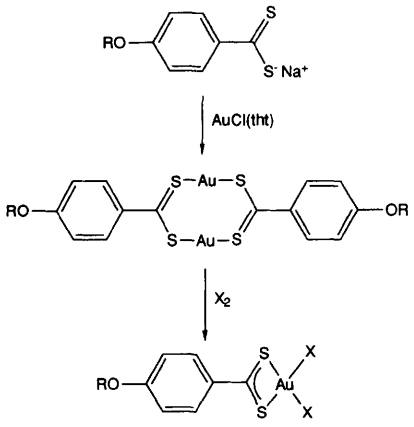

Scheme 2 Preparation of $[AuX_2(n\text{-odtb})]$

with elemental halogen to give the product in good yield (Scheme 2). The complex $[AuMe_2(8\text{-odtb})]$ was prepared by reaction of MeMgI with $[AuBr_2(8\text{-odtb})]$.

Palladium

The palladium complexes $[Pd(n\text{-odtb})_2]$ were synthesised according to the methods of Furlani and Luciani[12] by stirring an excess of the sodium salt of the acid in water with $[PdCl_4]^{2-}$ for *ca.* 3 h. This gave a dark precipitate which was washed and dried before being crystallised from hot toluene to give the desired product in typically 80% yield. The complexes were sparingly soluble in all solvents tried and so routine characterisation relied on IR spectroscopy and elemental microanalysis. While good analyses could be obtained for carbon and hydrogen, sulphur analyses proved much less reliable. A ^1H NMR spectrum was obtained for $[Pd(8\text{-odtb})_2]$ in toluene at 60 °C which showed the expected AA'XX' spin system for the benzene ring and a triplet at δ 4.0, characteristic of CH_2 attached to oxygen; the integration was also consistent with the proposed structure (Fig. 2).

These complexes were obtained as powders, deep-red for shorter chain lengths ($n \leqslant 7$) and green for longer alkoxy chain lengths. On heating the green complexes either as solids or in trying to dissolve them, the colour changed to red. The solid-state transition was observed by DSC which showed an endothermic transition at 59 °C with $\Delta H = 19.0$ kJ mol^{-1} for $[Pd(8\text{-odtb})_2]$ which was irreversible. The structure of the red isomer was confirmed by single-crystal X-ray studies on the octyloxy derivative which was found to be monomeric with D_{2h} symmetry about each palladium (see below). This complex had been initially obtained as a green powder, but red crystals formed on crystallisation from hot toluene. Small spectroscopic differences between the red and green forms were found in the ν_{CSS} region of their IR spectra where absorptions at 970 and 944 cm^{-1} (red isomer) and 972 and 948 cm^{-1} (green) were of quite different relative intensities. In solution, the electronic spectra measured in $CHCl_3$ showed no appreciable differences.

In the absence of direct evidence for the structure of the green isomer, we tentatively assign it as a dimeric species, $[Pd_2(n\text{-odtb})_4]$ with bridging dithiobenzoate ligands (Fig. 3).

This proposal is based on extensive work on related dithioacetate complexes[13–15] of Ni, Pd and Pt, many of which are known to exist in a number of structural forms. For

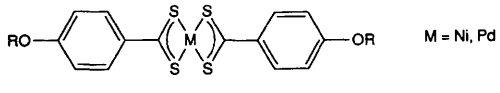

Fig. 2 Structure of the nickel and palladium complexes

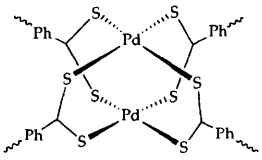

Fig. 3 Proposed structure for the green isomer of $[Pd(n\text{-odtb})_2]$

materials of the stoichiometry $[Pd(MeCS_2)_2]$, there are three distinct forms of which two have been crystallographically characterised.[15] The two characterised forms are a red isomer containing stacked monomeric (D_{2h}) and dimeric palladium units and a green form containing only dimeric units. The purely dimeric green form was observed to convert slowly to a red form if left exposed to air over a period of several days.

Nickel

Preparation of $[Ni(n\text{-odtb})_2]$ was achieved by dropwise addition of an aqueous solution of $NiCl_2$, in an inert atmosphere, to an aqueous solution containing an excess of the sodium salt of (*n*-odtb). After the solution had been stirred for 3 h, the resulting precipitate was recovered by filtration, washed, dried and crystallised from hot toluene to give the products as blue crystals in typically 70% yield. These nickel complexes are sparingly soluble and again, characterisation relied on IR spectroscopy and microanalytical data; sulphur analyses were again unhelpful. That these derivatives also had a planar, D_{2h} geometry was confirmed by the ^1H NMR spectrum obtained for $[Ni(8\text{-odtb})_2]$ in toluene at 60 °C, which gave a spectrum similar to that for the Pd complex with sharp lines, indicating that the complex was diamagnetic.

Zinc

The zinc complexes were obtained as orange powders in yields of *ca.* 60% by reaction of $[Zn(OAc)_2]$ with Na(*n*-odtb) in dilute acetic acid. These complexes were more soluble than their nickel and palladium analogues and osmometric molecular-weight measurements in toluene and chloroform showed them to be monomeric. By analogy with the unsubstituted bis(dithiobenzoato)zinc(II) which was shown by single-crystal studies to be monomeric in the solid state,[16] we expected that the alkoxydithiobenzoates of Zn^{II} would also be monomeric. However, single-crystal X-ray analysis of the butoxy and octyloxy derivatives showed them to be dimeric (see below). Dialkyldithiocarbamate complexes of Zn^{II} are also dimeric in the solid state and, in common with these new alkoxydithiobenzoates of Zn^{II}, exist as monomers in solution as shown by molecular-weight measurements.[17]

The nickel and palladium complexes, and to a lesser extent the zinc complexes, were highly coloured and were found to be highly dichroic in nematic solvents. The results of these studies are reported in the following paper.[18]

Phase Behaviour

The phase behaviour was determined using polarising optical microscopy, differential scanning calorimetry (DSC) and low-angle X-ray scattering.

Gold Complexes

The complexes prepared all showed an S_A phase (readily identified from the optical texture) at temperatures >100 °C (Table 1), regardless of chain length or the halogen. Unfortunately, all of the complexes began to decompose at, or just below, the clearing point. Replacement of the halogen by methyl reduced the melting point to *ca.* 60 °C, but lowered the thermal stability of the materials.

Table 1 Phase behaviour of [AuX_2(*n*-odtb)]

X	*n*	transition	*T*/°C	ΔH/kJ mol^{-1}	ΔS/J K^{-1} mol^{-1}
Cl	8	K–S_A	166	12.0	27.3
		S_A–I	198[a]	—	—
Cl	10	K–S_A	150	11.0	26.0
		S_A–I	200[a]	—	—
Br	8	K–S_A	145	20.6	49.2
		S_A–I	188[a]	—	—
Br	10	K–S_A	151	12.1	28.5
		S_A–I	190[a]	—	—
Me		K–S_A	60	—	—
		S_A–I	130[a]	—	—

[a] Decomposes.

The melting (and clearing) temperatures of these complexes were much lower than those of the Ni^{II} and Pd^{II} complexes which were also square planar. This lends further support to our idea[19] that lower symmetry complexes (Au = C_{2v}; Ni, Pd = D_{2h}) are expected to have lower melting points, probably due to less efficient packing of the molecules in the solid state.

Nickel and Palladium Complexes

The characterisation of these complexes by optical microscopy was very difficult because of their highly coloured natures. Phase assignments were therefore confirmed by X-ray scattering.

The mesomorphism of the two series was similar, with most homologues showing an S_C phase. In addition, three short-chain palladium homologues (*n* = 4–6) showed a nematic phase in addition to the S_C while the shortest-chain nickel homologue (*n* = 5) showed a nematic phase but no S_C. In general, the melting points of the palladium complexes were *ca.* 20–30 °C higher than those of the nickel complexes, whereas clearing points were *ca.* 80 °C higher. Many of the complexes showed some crystal polymorphism. As the clearing point was approached, decomposition was observed and in the case of palladium, thermogravimetric analysis (TG) showed that decomposition by weight loss began at this 'clearing' point.

In common with Ohta *et al.*,[9] a colour change from blue to red accompanying the decomposition of the nickel complexes was observed and although the decomposed product was not isolated, the nematic phase obtained at temperatures well below the clearing point of the materials was noted. Fackler and Coucouvanis[20] had shown previously that oxidation of bis(dithiobenzoato) complexes of Ni^{II} could lead to mixed dithiobenzoate–trithiobenzoate complexes. If such materials were formed on decomposition of these bis(alkoxydithiobenzoate)nickel(II) complexes, bent complexes would be formed [see Fig. 7(*a*) later] which would be expected to have lower clearing points than the parent material. We therefore undertook the synthesis of some alkoxytrithiobenzoate complexes which we found to be mesomorphic, with lower transition temperatures as predicted. The transition temperatures for the nickel and palladium complexes are given in Tables 2 and 3 and the phase diagrams are shown in Fig. 4 and 5.

Below the S_C phase of the materials were a number of very ordered phases, most of which were simply crystalline modifications. X-Ray scattering was used to investigate the phase immediately below the S_C which had been assigned previously as a crystal H phase by Ohta *et al.*[9]

Zinc Complexes

The phase behaviour of these complexes was less straightforward. The material obtained from the syntheses was an orange powder which analysed for the complex under investigation.

Table 2 Phase behaviour for [Ni(*n*-odtb)$_2$]

n	transition	*T*/°C	ΔH/kJ mol^{-1}	ΔS/J K^{-1} mol^{-1}
5	K–N	229	29.1	58.4
	N–I[a]	238	—	—
6	K–S_C	211	17.5	36.2
	S_C–I[a]	235	—	—
7	K–S_C	201	18.8	39.9
	S_C–I[a]	233	—	—
8	K–S[b]	155	10.5	27.8
	S[b]–S_C	192	14.3	29.6
	S_C–I[a]	230	—	—
9	K–S[b]	156	13.8	32.3
	S[b]–S_C	185	14.2	31.2
	S_C–I[a]	229	—	—
10	K–S[b]	145	15.6	37.4
	S[b]–S_C	174	11.2	25.1
	S_C–I[a]	230	—	—

[a] Transforms into red isotropic liquid; [b] S refers to an unidentified smectic phase (see text).

Table 3 Phase behaviour for [Pd(*n*-odtb)$_2$]

n	transition	*T*/°C	ΔH/kJ mol^{-1}	ΔS/J K^{-1} mol^{-1}
4	K–S_C	268	29.2	54.3
	S_C–N	278	4.9	9.0
	N–I	330	—	—
5	K–S_C	246	20.8	40.2
	S_C–N	297	8.3	14.6
	N–I	320	—	—
6	K–S_C	232	18.3	36.5
	S_C–N	307	9.0	15.5
	N–I	318	—	—
7	K–S_C	223	16.4	33.1
	S_C–I	317	—	—
8	K_{green}–K_{red}	59	19.0	57.2
	K_{red}–S[a]	107	15.6	41.4
	S[a]–S_C	215	12.7	26.2
	S_C–I	316	—	—
9	K_{green}–K_{red}	79	31.2	88.9
	K–S[a]	113	11.9	30.9
	S[a]–S_C	207	14.75	31.0
	S_C–I	315	—	—
10	K_{green}–K_{red}	75	24.4	70.0
	K–S[a]	114	15.2	39.4
	S[a]–S_C	201	13.5	28.7
	S_C–I	312	—	—

[a] S refers to an unidentified smectic phase (see text).

On careful crystallisation of this orange powder from toluene/hexane, red crystals were obtained which also analysed for the complex under investigation and which were used for the single-crystal structure determinations. The mesomorphism in these crystals was readily determined by optical microscopy in conjunction with DSC and it was found that all homologues showed a nematic phase. In addition, the nonyloxy and decyloxy homologues showed a S_C phase, while a monotropic S_C phase was observed for the octyloxy homologue. The transition temperatures for these materials are given in Table 4 and Fig. 6. Given that these crystals are dimers in the solid state but monomers in solution, it is not clear what the nature of the species in the mesophase might be. To answer this question, EXAFS experiments have been carried out[21] in both the solid state and the mesophase, as this technique can give good information of the co-ordination environment around the metal and has been used to good effect for the study of

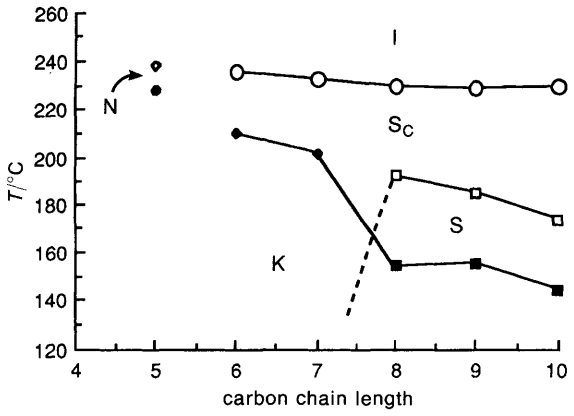

Fig. 4 Phase diagram for [Ni(*n*-odtb)$_2$]: ●, K–N; ◆, K–S$_C$; ○, S$_C$–I; ◇, N–I; ■, K–S$_X$; □, S$_X$–S$_C$

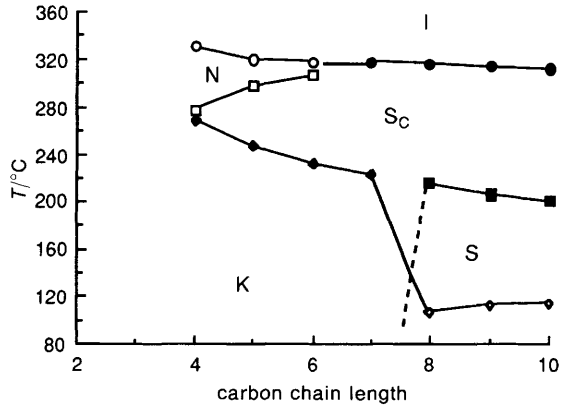

Fig. 5 Phase diagram for [Pd(*n*-odtb)$_2$]: ○, N–I; ◆, K–S$_C$; ●, S$_C$–I; ◇, K–S$_X$; ■, S$_X$–S$_C$; □, S$_C$–N

Table 4 Phase behaviour for [Zn$_2$(*n*-odtb)$_4$]

n	transition	*T*/°C	Δ*H*/kJ mol^{-1}	Δ*S*/J K^{-1} mol^{-1}
4	K–N	172	35.5	80.1
	N–I	201	—	—
5	K–N	152	29.6	70.4
	N–I	195	—	—
6	K–N	155	28.7	67.2
	N–I	194	—	—
7	K–N	158	32.3	74.9
	N–I	182	—	—
8	K–N	147	31.4	74.6
	N–I	184	—	—
	(N–S$_C$)	140	—	—
9	K–S$_C$	138	30.2	73.8
	S$_C$–N	155	4.0	9.3
	N–I	184	—	—
10	K–S$_C$	136	27.2	66.6
	S$_C$–N	164	3.9	9.0
	N–I	182	—	—

mesomorphic copper complexes.[22,23] The data from these experiments are still in the process of being evaluated.†

When the orange powders were examined, they showed that there were two materials present whose mesophases were immiscible. One of the mesophases was identified by its texture

† Note added in proof: Analysis of the data clearly shows that the dimer persists into the mesophase.

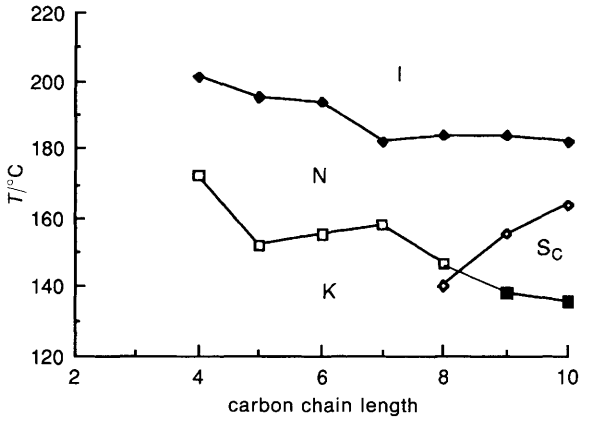

Fig. 6 Phase diagram for [Zn$_2$(*n*-odtb)$_4$]: □, K–N; ◆, N–I; ■, K–S$_C$; ◇, S$_C$–N

as nematic, while the other was found to be S$_C$; similar observations have been made for related complexes of cadmium and mercury.[24] The nature of the two materials is unclear, but it would appear that two different textures arise from two different crystal forms. Given that the red, crystalline form is known to be dimeric and that Bonamico has found a monomeric form for the unsubstituted bis(dithiobenzoato) zinc(II), it is possible that the two crystal forms which exist in the orange powder are monomer and dimer. EXAFS studies have also been carried out on these powders and the data are currently being evaluated.

Mesomorphic Trithiobenzoato Complexes

Complexes containing the alkoxytrithiobenzoate ligand (Fig. 7) were synthesised in an attempt to identify the materials formed by decomposition of the nickel complexes. The complexes were synthesised following the procedures described by Fackler and co-workers.[25] Thus, [Zn(8-ottb)$_2$] where 8-ottb = 4-octyloxytrithiobenzoato, was prepared in low yields (*ca.* 30%) by reaction of 4-alkoxybenzaldehyde, sulphur, ammonium sulphide and zinc chloride. Reaction of this complex with NiCl$_2$ led to a solution, from which [Ni(8-ottb)$_2$] and [Ni(8-ottb)(8-odtb)] could be isolated. However, [Ni(8-ottb)(8-odtb)] was more conveniently obtained by reaction of NiCl$_2$ with K8-odtb and K8-ottb in water. [Pd(8-ottb)(8-odtb)] was similarly obtained. Whereas the zinc complex was non-mesomorphic, all of the other complexes showed mesophases and our observations for [Ni(8-ottb)(8-odtb)] were essentially the same as those found for decomposed samples of [Ni(8-odtb)$_2$], supporting the idea that mesomorphic trithiobenzoate complexes are formed on decomposition and agreeing with similar studies by Ohta *et al.*[9] The transition temperatures for all the new complexes are given in Table 5. The reduced stability of both the crystal and nematic phases in these materials results from the reduced structural anisotropy compared with the corresponding dithiobenzoates.

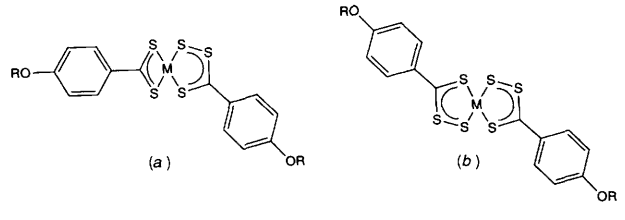

Fig. 7 Structure of the (*a*) [M(*n*-odtb)(*n*-ottb)] and (*b*) [M(*n*-ottb)$_2$] complexes

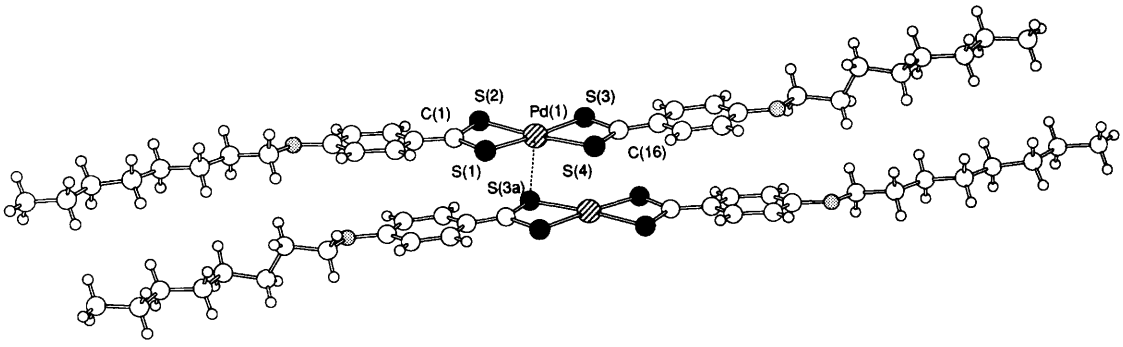

Fig. 8 Molecular structure of $[Pd(8\text{-odtb})_2]$

Table 5 Transition temperatures for the trithiobenzoate complexes

complex	transition	T/°C
[Ni(8-ottb)(8-odtb)]	K–N	126
	N–I	198
$[Ni(8\text{-ottb})_2]$	K–N	122
	N–I	186
	$(N–S_C)$	(95)
[Pd(8-ottb)(8-odtb)]	$K–S_C$	133
	$S_C–N$	161
	N–I	230

Table 6 Selected bond lengths for $[Pd(8\text{-odtb})_2]$[a]

bond	length/Å
Pd(1)—S(1)	2.293(12)
Pd(1)—S(2)	2.329(13)
Pd(1)—S(3)	2.304(12)
Pd(1)—S(4)	2.347(13)
Pd(1)---S(3a)	3.38
Pd(1)---Pd(1a)	3.94
S(1)—C(1)	1.723(25)
S(2)—C(1)	1.698(21)
S(3)—C(16)	1.717(27)
S(4)—C(16)	1.721(22)

[a] Estimated standard deviations in parentheses; the solid lines indicate that the two atoms are joined by a chemical bond, whereas the broken lines indicate a non-bonded interaction.

X-Ray Structural Investigations

Single Crystal Studies†

Crystal and Molecular Structure of $[Pd(8\text{-odtb})_2]$

The complex was recrystallised by allowing a saturated solution in toluene to cool slowly over a period of 24 h. The crystal structure was found to consist of discrete molecules which were weakly associated as dimers through metal–sulphur contacts. The molecular structure and packing are illustrated in Fig. 8 and 9, and selected bond lengths and angles are listed in Tables 6 and 7.

The molecule comprises a palladium which is chelated by two 4-octyloxydithiobenzoate ligands to give an approximate square-planar co-ordination geometry for the metal as indicated by the bond angles in Table 7. The planar geometry is slightly distorted towards square pyramidal by a displacement of the palladium of 0.058 Å from the mean plane (r.m.s. deviation 0.008 Å) through the four sulphur atoms. This is in contrast to the situation found for the unsubstituted complex $[Ni(S_2CC_6H_5)_2]$[26] where the Ni was buckled significantly out of plane. The S—Pd—S angles of 73.7(4) and 74.5(4)° showed a significant deviation from the ideal angle of 90° expected for a square-planar complex, but these angles, which are ascribed to the strain in the four-membered chelate, were almost identical to those found in the palladium complex of dithiobenzoic acid itself.[22] The angle between the two planar phenyl fragments is 5.5°. In each case, the substituent carbon and oxygen atoms are approximately coplanar with the ring (maximum deviation 0.053 Å). The dithiocarboxylate groups are twisted with respect to the adjacent phenyl planes by 8.0 and 6.0°, and with respect to each other by 2.5°. One octyloxyl chain shows closely antiperiplanar torsion angles between atoms O(1) and C(14) of +173, −178, 180, +179, +176, −175 and −175°: the other such chain contains two 'kinks' with torsion angles between atoms O(2) and C(29) of +169, +85, −176, −90, −168, +178 and +175°. The molecules are weakly associated in pairs across the crystallographic inversion centre at the origin of the unit cell where there is a pair of centrosymmetrically related Pd(1) ... S(3a) contacts of 3.38 Å (these form the axial sites in the square pyramid around the palladium): the shortest Pd ... Pd contact is 3.94 Å. The Ph—C distances (1.392–1.414 Å) indicate a partial double-bond character, which is consistent with the ligand planarity. The average C—S distance was 1.715(24) Å which indicates considerable multiple-bond character in the C—S bonds and consequently a lower electron density on the sulphur atoms (Table 6). All the geometrical features of the ligand were

† Supplementary data available from the Cambridge Crystallographic Data Centre: see Information for Authors, *J. Mater. Chem.*, 1991, Issue 1 or 4.

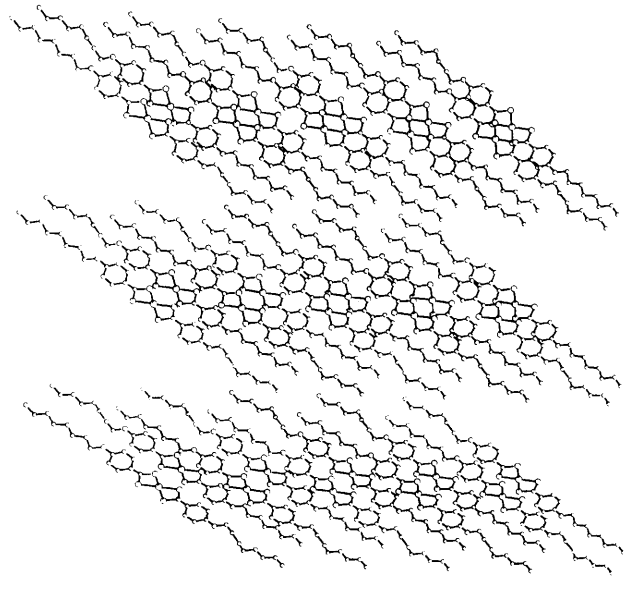

Fig. 9 Packing in $[Pd(8\text{-odtb})_2]$

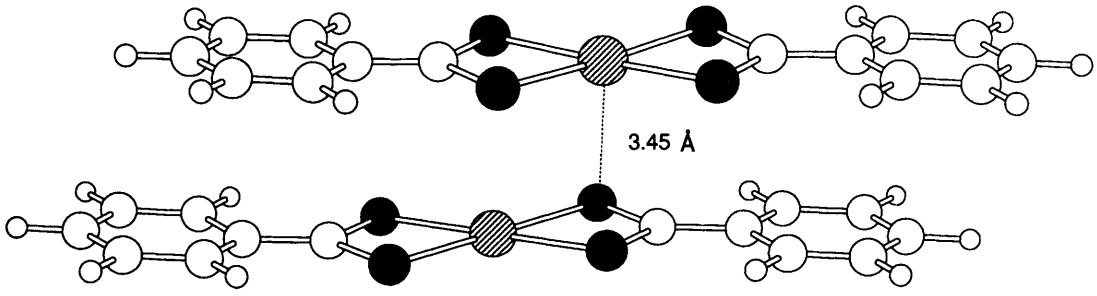

Fig. 10 Molecular structure of $[Pd(dtb)_2]$

Table 7 Selected bond angles for $[Pd(8\text{-}odtb)_2]$[a]

angle	angle/°
S(1)—Pd(1)—S(2)	74.5(4)
S(3)—Pd(1)—S(4)	73.7(4)
S(1)—Pd(1)—S(3)	176.6(4)
S(2)—Pd(1)—S(4)	175.6(4)

[a] Estimated standard deviations in parentheses.

Table 8 Selected bond lengths for $[Zn_2(4\text{-}odtb)_4]$[a]

bond	length/Å
Zn(1)—S(1)	2.770(6)
Zn(1)—S(2)	2.342(6)
Zn(1)—S(3)	2.326(6)
Zn(1)—S(4)	2.473(6)
Zn(1)—S(1a)	2.412(6)

[a] Estimated standard deviation in parentheses.

indicative of a high degree of conjugation in the core of the molecule.

The pairs of molecules lie parallel necessarily and form rafts parallel to the crystallographic *C* face. However, there is no clear separation between rafts, with the terminal carbon atoms of the chain forming a face separated from its neighbour by 0.24 Å only, and the terminal hydrogen centres interpenetrating the next raft. The angle between the longitudinal axis of the molecule [defined as the O(1) ... O(2) vector] and the normal to the face of the raft is 56°.

Many of the features found in the substituted palladium complexes are also evident in the crystal structure of the unsubstituted bis(dithiobenzoato)palladium(II) complex (Fig. 10), the first structural studies of which were made by Bonamico *et al.*[26] They found the structure to consist of monomers, weakly associated into trimers through metal–sulphur contacts; the metal co-ordination was reported to have remained essentially square-planar. That these substituted complexes are found to be associated into dimers only, is attributed to crystal packing constraints imposed by the presence of the alkoxy chains.

Crystal and Molecular Structure of $[\{Zn(4\text{-}odtb)_2\}_2]$

The complex was recrystallised by liquid diffusion in which a layer of hexane was placed on top of a concentrated solution of $[\{Zn(4\text{-}odtb)_2\}_2]$ in toluene. After 24 h, large needle-like crystals were formed at the interface and one of these was chosen for X-ray analysis.

The molecular structure is illustrated in Fig. 11, which shows that the molecule exists as centrosymmetric dimers, and that the zinc is in a five-co-ordinate environment with a geometry approximating to a trigonal bipyramid, in sharp contrast to the discrete monomeric units[15] found in the crystal structure of $[Zn(dtb)_2]$ (shown in Fig. 12). The dithiobenzoate chelate ligands each bridge between an axial and an equatorial site with subtended angles of 69 or 75°. The remaining equatorial site is occupied by a sulphur already occupying an axial site of an adjacent, centrosymmetrically related, zinc co-ordination polyhedron. Four of the five zinc–sulphur bonds, excluding that to the axial bridging sulphur [S(1)], are short, with the two shortest bonds to the equatorial sulphurs not involved in bridging. The longest 'normal' bond is to the non-bridging, axial sulphur atom, and the equatorial bond to the bridging sulphur is intermediate in length. These four short bonds are arranged approximately tetrahedrally, with a displacement of S(3) being the only significant distortion. Thus, the dimer is held together with one of the short zinc–sulphur bonds. The Zn(1)—S(1a) distance of 2.41 Å (Table 8) is comparable to the mean Zn—S distance of 2.40 Å in the four-membered chelate ring, showing that it is a strongly bonded dimer.

The two phenyl rings are each planar (r.m.s. deviations 0.004 and 0.007 Å) and are closely parallel (5.1°) and approximately coplanar. However, they are twisted with respect to the dithiocarboxylate residues by 14.4 and 5.3°, which are themselves mutually twisted by 24°. The zinc is displaced from these dithiocarboxylate residues by 0.48 and 0.47 Å: the oxygen atoms are essentially coplanar with the phenyl rings (deviations 0.043 and 0.003 Å), but C(12) is displaced from the adjacent phenyl ring by 0.091 Å. The terminal butoxy chains are antiperiplanar with all torsion angles within 5° of 180°.

The binuclear molecules necessarily lie parallel and form rafts (Fig. 13), parallel to the *C* face of the unit cell, which slightly overlap in projection, in contrast to some palladium and platinum complexes involving alkoxycyanobiphenyl ligands, where the rafts are well separated.[27] The longitudinal axis [defined as the vector between O(1) and O(2)] is at an angle of 62° to the normal to the raft.

Crystal and Molecular Structure of $[\{Zn(8\text{-}odtb)_2\}_2]$

The molecular structure is illustrated in Fig. 14. Each molecule exists as a centrosymmetric dimer with the zinc atom in a five-co-ordinate environment with a geometry which approximates to trigonal bipyramidal. The dithiobenzoate chelate ligands each bridge between an axial and an equatorial site with subtended angles of 69 or 75°. The remaining equatorial site is occupied by a sulphur already occupying an axial site of an adjacent, centrosymmetrically related, zinc co-ordination polyhedron. Four of the five zinc–sulphur bonds, excluding that to the axial bridging sulphur [S(1)], are short, with the two shortest bonds to the equatorial sulphurs not involved in bridging. The longest 'normal' bond is to the non-bridging, axial sulphur atom with the equatorial bond to the bridging sulphur intermediate in length. The four shortest bonds are arranged approximately tetrahedrally, with an inevitable 'pinching' displacement of S(3) being the only significant distortion [the angle between the Zn, S(3), S(4) and Zn, S(2),

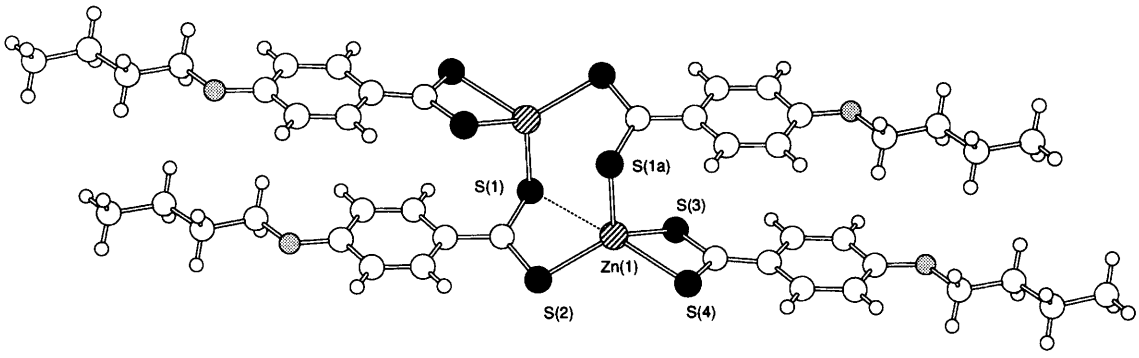

Fig. 11 Molecular structure of $[Zn_2(4\text{-odtb})_4]$

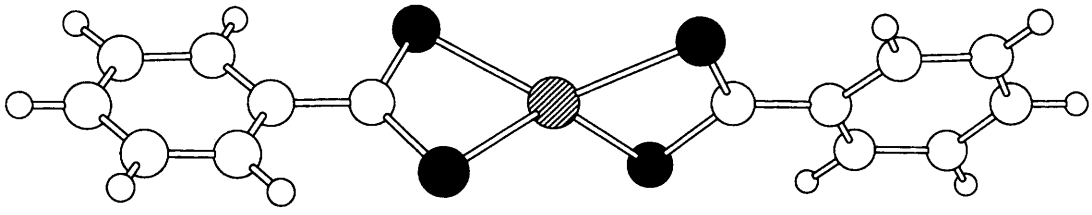

Fig. 12 Molecular structure of $[Zn(dtb)_2]$

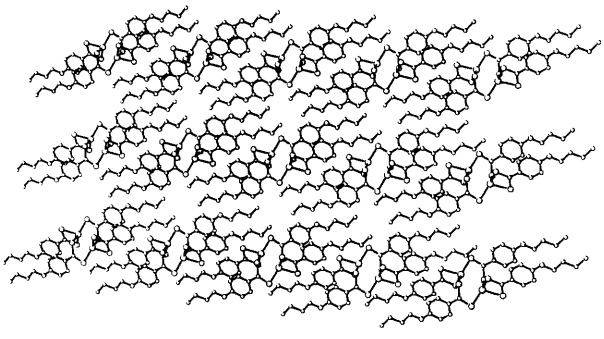

Fig. 13 Packing in $[Zn_2(4\text{-odtb})_4]$

Table 9 Selected bond angles for $[Zn_2(4\text{-odtb})_4]$[a]

angle	angle/°
S(1)—Zn(1)—S(2)	69.1(2)
S(1)—Zn(1)—S(3)	101.5(2)
S(2)—Zn(1)—S(3)	140.5(2)
S(1)—Zn(1)—S(4)	172.4(2)
S(2)—Zn(1)—S(4)	109.6(2)
S(3)—Zn(1)—S(4)	74.6(2)
S(1)—Zn(1)—S(1a)	85.4(2)
S(2)—Zn(1)—S(1a)	102.5(2)
S(3)—Zn(1)—S(1a)	115.3(2)
S(4)—Zn(1)—S(1a)	102.2(2)

[a] Estimated standard deviations in parentheses.

S(1a) planes is 85°]. Thus, the dimer is held together by one of the short zinc–sulphur bonds.

The two phenyl rings are each planar (r.m.s. deviations 0.017 and 0.011 Å) and are approximately parallel (8.4°), but stepped rather than coplanar. However, they are non-coplanar with respect to the dithiocarboxylate residues by 8.4 and 12.5° (respectively twisted/bent and twisted), which are themselves mutually inclined at 24°. The zinc is displaced from these dithiocarboxylate residues by 0.50 and 0.26 Å. The oxygen atoms are essentially coplanar with the phenyl rings (deviations 0.052 and 0.023 Å), but C(1) is displaced from the adjacent phenyl ring by 0.123 Å. The terminal octyloxy chains are antiperiplanar with all torsion angles within 5° of 180°.

The binuclear molecules necessarily lie parallel and form rafts parallel to the *C* face of the unit cell (Fig. 15), which significantly interpenetrate in projection, again in contrast to palladium and platinum complexes of alkoxycyanobiphenyl ligands where the rafts are well separated.[27] The longitudinal axis [defined as the vector between O(1) and O(2)] is at an angle of 77° to the normal to the raft.

The structure of the binuclear molecule shows a very close relationship to that of the corresponding complex carrying the shorter butoxy chains, although the molecular packing inevitably differs in detail. For example, the shortest non-bonding sulphur–sulphur contact between dimers in the octyloxy complex is 6.75 Å, whereas in the corresponding butoxy complex the shortest S ... S distance is 3.67 Å.

While the above structures are quite different from that observed for $[Zn(dtb)_2]$ itself, the eight-membered M—S—C—S—M—S—C—S ring is also found in the crystal structure of the diethyldithiocarbamate complexes[28–30] of Zn^{II}, Hg^{II} and Cd^{II}. In the case of the zinc complexes of the dithiocarbamates, solution molecular-weight measurements showed this complex to be monomeric and we also found this to be true for our zinc alkoxydithiobenzoates. Thus the intradimer Zn(1)—S(1a) bond at 2.41 Å is obviously relatively labile. The factors which control monomer/dimer formation in these systems are as yet unclear.

Low-angle Scattering Studies

Since the intense colour of the nickel and palladium complexes hindered phase identification by microscopy, the nature of their mesophases was investigated by small-angle X-ray scattering, using facilities at the Daresbury Laboratory and Bristol University. X-Ray diffraction patterns were recorded from powder samples using simultaneous X-ray diffraction/differential scanning calorimetry (XDDSC)[31] and also on flat-plate films.[32] The spectra obtained by the linear position sensitive detector from the XDDSC experiment on $[Pd(8\text{-odtb})_2]$ and $[Ni(8\text{-odtb})_2]$ are reproduced in Fig. 16 and 17, respectively.

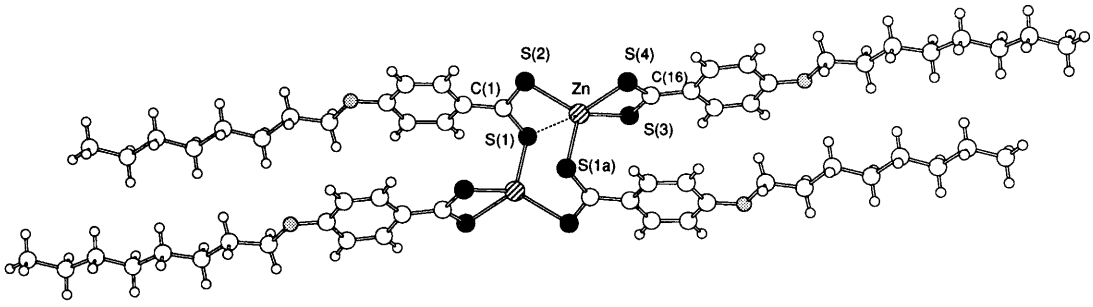

Fig. 14 Molecular structure of $[Zn_2(8\text{-odtb})_4]$

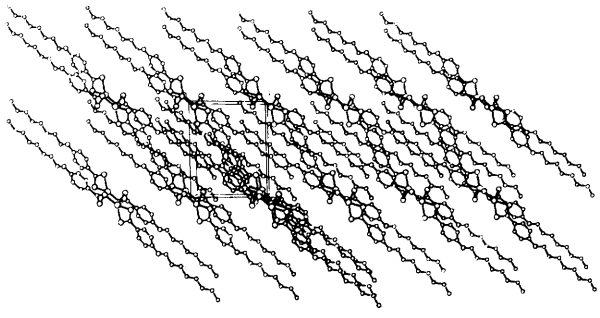

Fig. 15 Packing in $[Zn_2(8\text{-odtb})_4]$

Table 10 Selected bond lengths for $[Zn_2(8\text{-odtb})_4]$[a]

bond	length/Å
Zn—S(1)	2.837(9)
Zn—S(2)	2.345(8)
Zn—S(3)	2.360(8)
Zn—S(4)	2.500(8)
Zn—S(1a)	2.414(8)

[a] Estimated standard deviations in parentheses.

Table 11 Selected bond angles for $[Zn_2(8\text{-odtb})_4]$[a]

angle	angle/°
S(1)—Zn—S(2)	69.2(2)
S(1)—Zn—S(3)	96.6(2)
S(2)—Zn—S(3)	138.5(3)
S(1)—Zn—S(4)	165.2(2)
S(2)—Zn—S(4)	109.0(2)
S(3)—Zn—S(4)	75.0(2)
S(1)—Zn—S(1a)	87.4(2)
S(2)—Zn—S(1a)	102.6(2)
S(3)—Zn—S(1a)	115.9(2)
S(4)—Zn—S(1a)	107.1(2)

[a] Estimated standard deviations in parentheses.

In each complex the higher-temperature mesophase was found to be lamellar in nature with no in-plane correlations. Layer spacings (d) were found to be *ca.* 26 Å compared to a molecular length (l) of 39 Å from CPK models. With the assumption of no interdigitation of the layers, the tilt (β_t) of the molecules in the layers was estimated to be 48° from the equation:

$$\beta_t = \cos^{-1}(d/l)$$

Although this is consistent with an S_C phase (which also agrees with the microscopy), such a high tilt angle is unlikely to be observed and hence some interdigitation of the layers can be expected.

For each compound, the phase immediately below the S_C phase gave an optical texture essentially identical to that of the crystal smectic G phase and the diffraction patterns from the two compounds appeared identical. Ohta *et al.*[9] had previously suggested that this phase in the Ni complex was a crystal H phase. However, despite observing almost twice the number of reflections on flat-plate film, we were unable to derive a unique unit cell which would identify this phase. If it is assumed that the strongest peak at high Q is the {110} reflection, then the unit cell tilts like a crystal K phase with a bilayer structure; the presence of {100} and {101} reflections, however, implies that it may not be a rotator phase. Unambiguous assignment of the phase will therefore require diffrac-

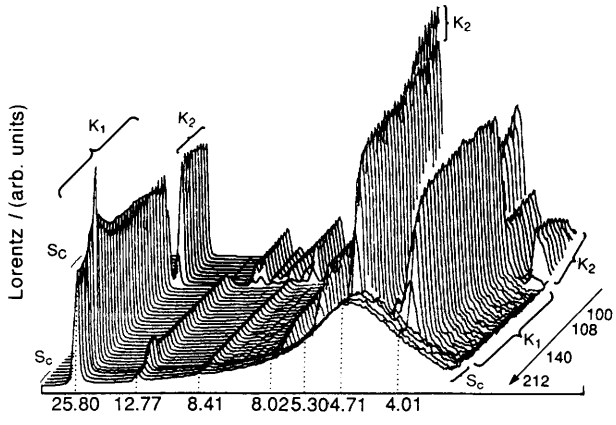

Fig. 16 X-Ray diffraction scan from $[Pd(8\text{-odtb})_2]$ on heating from 70 to 230 °C by XDDSC technique. The intensity (I) has been corrected for Lorentz and polarisation factors, the horizontal axis is the scattering vector (Q) (but the numbers refer to the d-spacing in Å) and each frame is the average of four spectra

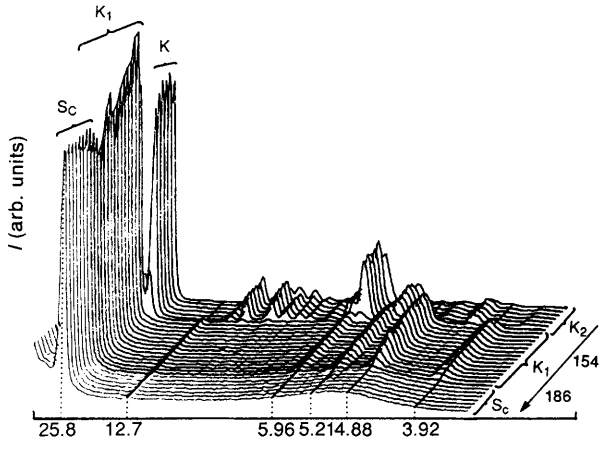

Fig. 17 X-Ray diffraction scan from $[Ni(8\text{-odtb})_2]$ on heating from 141 to 200 °C by XDDSC technique. The vertical scale is intensity (I) and the horizontal axis is the scattering vector (Q) (the numbers refer to the d-spacing in Å); each frame is the average of two spectra

tion studies from monodomain structures and so we cannot confirm (nor can we rule out) Ohta's assignment as a crystal H phase.

Experimental

Microanalyses were performed by the University of Sheffield. All chemicals were used as received unless otherwise specified. IR spectra were recorded on Perkin–Elmer PE1579 (4000–625 cm^{-1}), PE684 (400–200 cm^{-1}) and PE1710 (4400–600 cm^{-1}) spectrometers. Spectra were recorded as Nujol mulls between NaCl plates or polythene plates, or as KBr discs. ^1H NMR spectra were recorded on a Bruker WM250 spectrometer; proton chemical shifts are quoted relative to internal $CDCl_3$. Mass spectra were recorded on a Kratos MS25 instrument with a DS55 data system. Mesomorphism was studied by heated-stage polarising microscopy using a Zeiss Labpol microscope equipped with a Linkam TH600 hot-stage and PR600 temperature controller. The heating rate used was in the range 0.5–10.0 K min^{-1}. Once transition temperatures had been determined, heats of transition were measured by differential scanning calorimetry, which was carried out using a Perkin-Elmer DSC7 instrument. Molecular weights were obtained using a Knauer vapour pressure osmometer with benzil as standard.

Solvents

Where necessary, solvents were dried prior to use according to standard methods. Carbon disulphide, acetone and diethyl ether were stored over molecular sieves (3 Å) for 3 days prior to use. Tetrahydrofuran, toluene and diethyl ether were freshly distilled from sodium–benzophenone prior to use. Solvents used for reactions involving air-sensitive species were thoroughly outgassed prior to use and manipulations were carried out using standard Schlenk line and catheter tubing techniques.

Synthesis

Unless stated otherwise all reactions in these preparations were performed under an atmosphere of argon and were carried out as described below for the octyloxy derivative.

Preparation of 4-Octyloxydithiobenzoic Acid

The Grignard reagent obtained from the reaction of 4-octyloxybromobenzene (16 g, 56.1 mmol) with vacuum-dried magnesium turnings (1.4 g, 57.6 mmol) in THF (50 cm^3) was allowed to cool to room temperature with stirring and was then filtered into a dry flask which was surrounded by a mixture of ice and salt (−10 °C). Carbon disulphide (3.5 cm^3, 57.6 mmol) was transferred by syringe to a dropping funnel and was added dropwise to the filtrate with stirring so that the temperature did not rise above 0 °C. When the addition was complete, stirring was continued for *ca.* 3 h at 0 °C, after which the ice-bath was removed and the reaction product allowed to stand at room temperature for *ca.* 1 h with stirring. The following stages were performed in air. The solution was poured onto ice (150 g) which was then acidified with dilute hydrochloric acid (25 cm^3, 1 mol dm^{-3}). The product was extracted into diethyl ether (75 cm^3) to give a deep-red solution which was then extracted with portions of aqueous sodium hydroxide (3 × 20 cm^3, 5% w/v) until the diethyl ether layer retained only slight colouration; this gave an aqueous solution of the orange sodium salt of the acid which was then separated from the diethyl ether. The free dithiobenzoic acid was re-extracted into diethyl ether (100 cm^3) after acidification with dilute hydrochloric acid (30 cm^3; 1 mol dm^{-3}) until the aqueous solution retained only slight colouration. This interconversion of the sodium salt and the free acid was repeated three or four times to purify the acid.

Finally, an ethereal solution of the dithiobenzoic acid was washed with water (3 × 30 cm^3) and dried over magnesium sulphate. The solution was then reduced in volume to *ca.* 10 cm^3 and left overnight in a freezer at −25 °C. This yielded dark-red crystals which were recovered by filtration and air-dried: yield 10.56 g, 66%. The purified product was then converted to its more stable sodium salt and stored under an atmosphere of argon in the dark.

Preparation of Bis(4-Octyloxydithiobenzoato)nickel(II)

To a stirred solution of sodium 4-octyloxydithiobenzoate (0.5 g, 1.64 mmol) in water (25 cm^3) was added dropwise a pale-green solution of $NiCl_2 \cdot 6H_2O$ (0.12 g, 0.5 mmol) in water (10 cm^3) at room temperature. An immediate dark-blue precipitate formed which was left to stir for *ca.* 3 h. The mixture was filtered, washed with water (2 × 10 cm^3) and acetone (2 × 5 cm^3) and dried. On crystallisation from hot toluene, the product was recovered as dark-blue crystals which were filtered off, washed with diethyl ether and dried. Yield 239 mg, 77%. We obtained similar IR spectra to those reported by Ohta *et al.*,[9] but assigned $\nu_{(CSS)_{asymm}}$ and $\nu_{(CSS)_{symm}}$ at 977 and 948 cm^{-1} respectively after the detailed work of Maltese.[34] EI mass spectrum *m/z* 620 $[Ni(S_2CC_6H_4OC_8H_{17})_2]^+$. Microanalytic data are given in Table 12.

Preparation of Bis(4-Octyloxydithiobenzoato)palladium(II)

To a stirred solution of sodium 4-octyloxydithiobenzoate (0.83 g, 2.73 mmol) in water (20 cm^3), was added dropwise a dark-brown solution of Na_2PdCl_4 (0.25 g, 0.85 mmol) in water (10 cm^3) at room temmperature. A precipitate formed immediately and the mixture was left to stir for *ca.* 3 h. The green solid was recovered by filtration, washed with water (2 × 10 cm^3) and then with diethyl ether (2 × 5 cm^3) and finally recrystallised from hot toluene to give red crystals which were filtered off, washed with diethyl ether and dried *in vacuo*: yield 483 mg, 85%. EI mass spectrum *m/z* 668 $[Pd(S_2CC_6H_4OC_8H_{17})_2]^+$. Microanalytical data are given in Table 13.

Preparation of Bis(4-Octyloxydithiobenzoato)zinc(II)

To a stirred solution of sodium 4-octyloxydithiobenzoate (0.2 g, 0.63 mmol) in water (20 cm^3) was added acetic acid (glacial) until the solution pH had dropped to 3. A solution of $Zn(OAc)_2 \cdot 2H_2O$ (0.06 g, 0.27 mmol) in water (10 cm^3) acidified with acetic acid was added dropwise, resulting in the immediate formation of an orange precipitate. Stirring was continued for 8 h after which the precipitate was recovered by filtration, washed well with water and dried *in vacuo*. The orange solid (0.15 g, 88%) was analytically pure. The red crystalline solids referred to in the text were then obtained by diffusion of hexane into concentrated toluene solutions of

Table 12 Experimental data for bis(4-alkoxydithiobenzoato)nickel(II)

complex	yield (%)	microanalysis found (calculated) (%) C	H
$[Ni(4\text{-odtb})_2]$	83	52.0 (51.9)	5.3 (5.1)
$[Ni(5\text{-odtb})_2]$	85	53.6 (53.6)	5.9 (5.6)
$[Ni(6\text{-odtb})_2]$	88	55.0 (55.2)	6.0 (6.1)
$[Ni(7\text{-odtb})_2]$	86	55.6 (56.7)	6.3 (6.5)
$[Ni(8\text{-odtb})_2]$	77	57.2 (57.9)	6.9 (6.8)
$[Ni(9\text{-odtb})_2]$	84	58.9 (59.2)	6.9 (7.1)
$[Ni(10\text{-odtb})_2]$	73	60.5 (60.3)	7.3 (7.4)

Table 13 Experimental data for bis(4-alkoxydithiobenzoate)palladium(II)

complex	yield (%)	microanalysis found (calculated) (%) C	H
$[Pd(4\text{-odtb})_2]$	79	47.0 (47.4)	4.5 (4.7)
$[Pd(5\text{-odtb})_2]$	78	49.0 (49.3)	5.0 (5.2)
$[Pd(6\text{-odtb})_2]$	73	50.9 (50.9)	5.7 (5.6)
$[Pd(7\text{-odtb})_2]$	88	52.0 (52.5)	5.9 (5.9)
$[Pd(8\text{-odtb})_2]$	85	53.4 (53.8)	6.5 (6.3)
$[Pd(9\text{-odtb})_2]$	76	54.7 (55.1)	6.6 (6.7)
$[Pd(10\text{-odtb})_2]$	78	56.9 (56.3)	6.9 (6.9)

the complexes at room temeprature. Microanalytical data are given in Table 14.

Preparation of (4-*Octyloxydithiobenzoatodichloro*)*gold*(III)
A solution of H8-odtb (0.35 g) in diethyl ether (10 cm^3) was extracted with a solution of sodium hydroxide. This aqueous solution was then added slowly to a solution of (tetrahydrothiophene)gold chloride (0.2 g) in acetone (20 cm^3), giving a brown–violet solid. After 3 h stirring, the solid was filtered off and washed with ethanol, water and then diethyl ether.

Chlorine was then bubbled through a suspension of this solid, $[Au_2(8\text{-odtb})_2]$, in $CHCl_3$ until the solution was yellow–orange. The volume of the solution was then reduced and diethyl ether added to precipitate the product which was filtered and washed with diethyl ether: yield 69%. Other derivatives were prepared in a similar way. A slight excess of bromine was used to make the dibromides.

Preparation of (4-*Octyloxydithiobenzoatodimethyl*)*gold*(III)
To a solution of MeMgI (1.16 mmol) in diethyl ether was added $[AuBr_2(8\text{-odtb})]$ (0.3 g). After 15 min, undried diethyl ether was added (10 cm^3) and then all solvent was removed. The residue was extracted with dichloromethane (50 cm^3) which was then removed. The product was crystallised from the extracted solid in cold diethyl ether: yield 25%. Microanalytical data are given in Table 15.

Table 14 Experimental data for tetrakis(4-alkoxydithiobenzoato)dizinc(II)

complex	yield (%)	microanalysis found (calculated) (%) C	H
$[Zn(4\text{-odtb})_2]$	83	51.1 (51.2)	5.4 (5.1)
$[Zn(5\text{-odtb})_2]$	87	55.9 (55.9)	5.5 (5.6)
$[Zn(6\text{-odtb})_2]$	76	54.4 (54.6)	5.8 (6.0)
$[Zn(7\text{-odtb})_2]$	67	55.9 (56.0)	6.2 (6.4)
$[Zn(8\text{-odtb})_2]$	88	57.1 (57.4)	6.6 (6.7)
$[Zn(9\text{-odtb})_2]$	91	58.4 (58.6)	6.9 (7.0)
$[Zn(10\text{-odtb})_2]$	93	58.9 (59.7)	7.3 (7.4)

Table 15 Experimental data for (4-alkoxydithiobenzoato)gold(III) complexes

X	*n*	yield (%)	microanalysis found (calculated) (%) C	H
Cl	8	69	33.2 (32.6)	4.1 (3.8)
Cl	10	62	36.0 (35.4)	4.6 (4.4)
Br	8	45	28.4 (28.1)	3.7 (3.3)
Br	10	74	30.1 (30.7)	4.0 (3.8)
Me	8	25	40.1 (40.0)	5.9 (5.3)

Preparation of Bis(*octyloxytrithiobenzoato*)*zinc*(II)
To a mixture containing sulphur (0.3 g), aqueous ammonium sulphide (4.02 cm^3, 16%) in THF (20 cm^3) was added dropwise a solution of 4-octyloxybenzaldehyde (2.2 g) in THF (10 cm^3). The mixture was refluxed for 20 min and then cooled in an ice bath. A solution of $ZnCl_2$ (0.32 g) in water (10 cm^3) was then added, followed by water to bring the total volume to *ca.* 100 cm^3. On stirring over 30 min, an orange oil appeared. The aqueous layer was decanted off and the oil triturated with MeOH, causing solidification. The MeOH was separated and the precipitate washed with hydrochloric acid (50 cm^3, 10%) and then again with MeOH. Acetone was added to the solid which was recovered by filtration, washed with acetone and air-dried. The product was recrystallised from $CHCl_3$/light petrol. Yield 30%.

Preparation of Bis(*octyloxytrithiobenzoato*)*nickel*(II)
To a solution of $[Zn(8\text{-ottb})_2]$ (0.5 g) in THF (20 cm^3) was added a solution of $NiCl_2 \cdot 6H_2O$ (0.185 g) in MeOH (10 cm^3). After 2 min, water was added to the dark solution and a dark precipitate appeared which was filtered off, washed with water and air-dried. The crude product was dissolved in $CHCl_3$ (leaving a dark-green residue) and the volume of the solution was reduced to *ca.* 5 cm^3 leading to the dark-violet product in 39% yield. Addition of *n*-pentane to the mother liquor precipitated the remaining material as a 1:1 mixture (by NMR) of $[Ni(8\text{-ottb})_2]$ and [Ni(8-ottb)(8-odtb)].

Preparation of (4-*Octyloxytrithiobenzoato*)(4-*octyloxydithiobenzoato*)*nickel*(II)
A solution containing sulphur (0.122 g) and aqueous ammonium sulphide (3.26 cm^3, 16%) in ethanol (30 cm^3) was added dropwise to a solution of 4-octyloxybenzaldehyde (1.66 g) in ethanol (10 cm^3). The reaction mixture was refluxed for 5 min, turning deep red. The mixture was cooled to room temperature using an ice bath and a colourless solid was removed by filtration.

A solution of concentrated hydrochloric acid (20 cm^3) in water (100 cm^3) was then added to the red solution generated above and a crude mixture of 4-octyloxyperthiobenzoic acid and 4-octyloxydithiobenzoic acid was extracted with diethyl ether (3×30 cm^3). The diethyl ether layer was then shaken with a solution of KOH (7.5 g) in water (150 cm^3). This aqueous layer was separated and then neutralised with hydrochloric acid.

To this aqueous solution was added a solution of $NiCl_2 \cdot 6H_2O$ (0.455 g) in water (15 cm^3). The blue–violet precipitate formed was filtered, washed with ethanol and air-dried. The crude product was dissolved in THF and the volume reduced to 2 cm^3 before acetone was added to precipitate the dark-violet product: yield 8%.

Preparation of (4-*Octyloxyperthiobenzoato*)(4-*octyloxydithiobenzoato*)*palladium*(II)
A solution of $K_2[PdCl_4]$ (0.31 g) in water (10 cm^3) was added to a neutral solution of the potassium salts of 4-octyloxytri-

Table 16 Analytical data for the trithiobenzoate complexes

complex	yield (%)	microanalysis found (calculated) (%) C	H
$[Zn(8\text{-ottb})_2]$	30	52.1 (52.0)	6.0 (6.1)
[Ni(8-ottb)(8-odtb)]	8	55.1 (55.2)	7.2 (7.0)
$[Ni(8\text{-ottb})_2]$	39	52.7 (52.5)	6.1 (6.2)
[Pd(8-ottb)(8-odtb)]	15	50.9 (51.3)	6.0 (6.2)

Table 17 Crystal data

parameter	[Pd(8-odtb)$_2$]	[Zn$_2$(4-odtb)$_4$]	[Zn$_2$(8-odtb)$_4$]
molecular formula	[$C_{30}H_{42}O_2S_4Pd$]	[$C_{44}H_{52}O_4S_8Zn_2$]	[$C_{60}H_{84}O_4S_8Zn_2$]
M_r/g mol^{-1}	669.30	1032.14	1256.58
crystals from	toluene	toluene/hexane	toluene/hexane
crystal dimensions/mm	0.9 × 0.175 × 0.05	0.7 × 0.075 × 0.075	0.6 × 0.6 × 0.15
appearance	red	red/orange	red
crystal system	triclinic	triclinic	triclinic
a/Å	8.068(34)	8.106(16)	10.475(34)
b/Å	9.744(14)	12.395(11)	12.853(33)
c/Å	20.412(11)	12.382(23)	12.481(23)
α/°	85.83(33)	87.56(12)	89.08(21)
β/°	88.07(40)	78.99(15)	103.89(22)
γ/°	82.46(25)	71.38(13)	89.10(22)
U/Å^3	1586	1157	1631
D_c/g cm^{-3}	1.40	1.48	1.28
Z	2	1	1
space group	$P\bar{1}$ (C_i^1, no. 2)	$P\bar{1}$ (C_i^1, no. 2)	$P\bar{1}$ (C_i^1, no. 2)
μ(Mo-Kα)/cm^{-1}	8.54	14.49	10.40
F(000)	695.94	535.93	663.91
measured reflections	5817	4154	5777
independent reflections	2201	2163	2014
azimuthal scans	4	10	5
transmission coeff.: min., max.	0.584, 0.628	0.844, 0.897	0.349,0.394
R	0.1178	0.0865	0.1328
no. of parameters	312	262	334
final δ/σ: mean, max.	0.016, 0.189	0.003, 0.012	0.038, 0.145

Table 18 Atomic coordinates (×10^4) and temperature factors for [Pd(8-odtb)$_2$]

atom	x	y	z	$10^3\ U_{eq}$[a]/Å^2
Pd(1)	1590(3)	1156(2)	−441(1)	57(1)
S(1)	1516(10)	3488(8)	−328(4)	90(3)
S(2)	3500(10)	1332(7)	370(4)	92(3)
S(3)	1833(10)	−1197(7)	−558(4)	88(3)
S(4)	−175(10)	859(7)	−1297(4)	92(3)
O(1)	5490(23)	6730(23)	1828(11)	102(10)
O(2)	−1558(26)	−4743(24)	−2762(10)	117(11)
C(1)	2922(28)	3074(20)	295(11)	75(11)
C(2)	3526(19)	4061(14)	669(8)	54(9)
C(3)	3161(19)	5485(14)	514(8)	76(11)
C(4)	3800(19)	6422(14)	891(8)	87(13)
C(5)	4804(19)	5935(14)	1424(8)	75(11)
C(6)	5168(19)	4512(14)	1579(8)	80(12)
C(7)	4529(19)	3575(14)	1202(8)	99(14)
C(8)	5280(40)	8154(28)	1780(14)	122(18)
C(9)	6107(41)	8493(11)	2387(13)	137(20)
C(10)	5937(48)	10019(11)	2432(14)	174(25)
C(11)	6751(40)	10397(11)	3033(12)	144(21)
C(12)	6536(40)	11943(10)	3027(10)	140(20)
C(13)	7190(50)	12462(19)	3625(14)	148(22)
C(14)	6756(58)	14016(21)	3584(16)	209(32)
C(15)	7515(87)	14611(32)	4137(23)	501(80)
C(16)	414(30)	−902(21)	−1176(12)	93(13)
C(17)	−21(22)	−1883(17)	−1580(9)	84(13)
C(18)	524(22)	−3286(17)	−1430(9)	75(11)
C(19)	43(22)	−4285(17)	−1815(9)	65(10)
C(20)	−983(22)	−3880(17)	−2350(9)	84(13)
C(21)	−1527(22)	−2477(17)	−2500(9)	96(14)
C(22)	−1046(22)	−1479(17)	−2115(9)	85(13)
C(23)	−1092(35)	−6170(30)	−2660(14)	112(16)
C(24)	−2050(43)	−7020(43)	−3055(16)	174(27)
C(25)	−1300(48)	−7169(39)	−3724(15)	291(50)
C(26)	−2336(50)	−7946(28)	−4126(18)	209(34)
C(27)	−1770(59)	−9470(26)	−4040(18)	193(33)
C(28)	−2543(51)	−10207(23)	−4549(19)	175(28)
C(29)	−1927(55)	−11723(24)	−4479(21)	217(35)
C(30)	−2805(51)	−12479(28)	−4943(20)	253(39)

[a] Equivalent isotropic U defined as one third of the trace of the orthogonalised U_{ij} tensor.

thiobenzoic acid and 4-octyloxydithiobenzoic acid prepared as described above. A dark-brown precipitate developed immediately and after stirring for 1 h, the precipitate was filtered, washed with ethanol and air-dried. The crude product was dissolved in $CHCl_3$, the volume of the solution reduced to *ca.* 5 cm^3 and then cooled to give a red–violet product in 15% yield. Microanalytical data are given in Table 16.

Crystal Structure Determination

Three-dimensional room-temperature X-ray data were collected on a Nicolet *R3m* diffractometer in the range $3.5° < 2\theta < 50°$ by the ω-scan method using Mo-Kα radiation ($\lambda = 0.71069$ Å). The independent reflections for which $|F|/\sigma(|F|) > 3.0$ were corrected for Lorentz and polarisation effects, and for absorption by analysis of azimuthal scans (minimum and maximum transmission coefficients as in Table 17). The structures were solved by standard Patterson and Fourier techniques and refined by blocked cascade least-squares methods. Hydrogen atoms were placed in calculated positions and their isotropic thermal parameters were related to those of the supporting carbon atom. Complex scattering factors were obtained from a standard source[34] and from the program package SHELXTL[35] as implemented on the Data General Nova 3 computer.

Bis(octyloxydithiobenzoato)palladium(II)

Geometric constraints were applied to each of the two phenylene rings (D_{6h} symmetry C—C 1.395 Å) and their four hydrogen atoms; the four S—C bonds were constrained to be equal; the C—C bonds in the terminal octyl chains were constrained to be equal and the C—C—C angles were constrained to be close-to-normal tetrahedral values. The refinement converged at $R = 0.1178$ with allowance for thermal anisotropy of all non-hydrogen atoms. A final-difference electron-density synthesis showed minimum and maximum values of −1.26 and +0.90 Å^{-3}. Unit weights were used throughout the refinement. Table 18 shows atomic positional parameters with estimated standard deviations.

Tetrakis(butoxydithiobenzoato)dizinc(II)

The refinement converged at $R=0.0865$ with allowance for thermal anisotropy of all non-hydrogen atoms. A final-difference electron-density synthesis showed minimum and maximum values of -0.72 and $+0.63$ e Å^{-3}. Unit weights were used throughout the refinement. Table 19 has atomic positional parameters with estimated standard deviations.

Tetrakis(octyloxydithiobenzoato)dizinc(II)

Hydrogen atoms were included in calculated positions, with isotropic thermal parameters related to those of the supporting atom, and refined in riding mode. Refinement converged at a final R of 0.1328 (R_w 0.0887), with allowance for the thermal anisotropy of all non-hydrogen atoms. A final-difference electron-density synthesis showed minimum and maximum values of -0.71 and $+0.90$ e Å^{-3}. A weighting scheme $w^{-1}=[\sigma^2(F)+0.00010(F)^2]$ was used in the latter stages of the refinement. Table 20 has atomic positional parameters with estimated standard deviations.

X-Ray Scattering Experiments

X-Ray scattering experiments using XDDSC[32] or flat-plate films[33] were carried out as previously described; XDDSC experiments were performed using synchrotron radiation at $\lambda=1.54$ Å. Scans were made at 1° intervals, although the plots show traces averaged over 4° (*i.e.* four spectra) for Pd (Fig. 16) and 2° (two spectra) for Ni (Fig. 17). In addition, diffraction patterns from powder samples in Lindemann tubes were obtained at selected temperatures and were recorded on flat plate films using synchrotron radiation ($\lambda=1.54$ Å) and also using a conventional sealed source tube (Cu-Kα radiation).

Table 19 Atomic coordinates ($\times10^4$) and temperature factors for $[Zn_2(4\text{-odtb})_4]$

atom	x	y	z	$10^3\ U_{eq}$[a]/Å^2
Zn(1)	1060(2)	982(1)	550(1)	49(1)
S(1)	1540(5)	−1309(3)	255(3)	45(1)
S(2)	301(7)	151(3)	2228(3)	65(2)
S(3)	3530(5)	1194(3)	−634(3)	51(1)
S(4)	1019(5)	2942(3)	889(3)	51(1)
O(1)	−1892(13)	−4348(7)	4081(8)	61(4)
O(2)	5478(12)	5808(7)	−2468(7)	56(4)
C(1)	543(17)	−1068(11)	1618(10)	41(5)
C(2)	−83(17)	−1965(10)	2254(10)	40(5)
C(3)	430(18)	−3070(10)	1857(11)	45(5)
C(4)	−148(18)	−3878(11)	2422(10)	48(6)
C(5)	−1285(19)	−3590(11)	3441(12)	52(6)
C(6)	−1829(19)	−2493(11)	3851(11)	51(6)
C(7)	−1240(19)	−1688(11)	3275(10)	50(6)
C(8)	−1314(20)	−5503(11)	3739(11)	53(6)
C(9)	−2165(21)	−6154(11)	4586(12)	59(7)
C(10)	−1587(25)	−7400(12)	4281(12)	72(8)
C(11)	−2415(25)	−8102(13)	5114(14)	79(8)
C(12)	2711(16)	2588(10)	−218(10)	39(5)
C(13)	3470(18)	3409(10)	−758(10)	39(5)
C(14)	2918(19)	4529(11)	−386(11)	54(6)
C(15)	3533(18)	5367(11)	−941(11)	50(6)
C(16)	4789(16)	5052(11)	−1880(10)	41(5)
C(17)	5396(18)	3933(11)	−2270(11)	53(6)
C(18)	4734(19)	3145(12)	−1717(11)	55(6)
C(19)	4867(18)	6964(10)	−2118(11)	47(6)
C(20)	5735(18)	7633(11)	−2939(11)	48(5)
C(21)	5173(21)	8860(11)	−2636(11)	57(6)
C(22)	5891(23)	9583(12)	−3473(14)	78(8)

[a] Equivalent isotropic U defined as one third of the trace of the orthogonalised U_{ij} tensor.

Table 20 Atomic coordinates ($\times10^4$) and temperature factors for $[Zn_2(8\text{-odtb})_4]$

atom	x	y	z	10^3U_{eq}[a]/Å^2
Zn	799(2)	638(2)	1356(2)	78(1)
S(1)	−1660(5)	540(3)	−204(4)	73(2)
S(2)	−660(5)	−409(4)	2031(4)	92(3)
S(3)	1145(5)	2423(3)	1085(4)	82(2)
S(4)	2673(5)	1095(3)	2923(4)	89(3)
O(1)	−5913(11)	−3259(8)	109(8)	98(6)
O(2)	6051(10)	5524(7)	3307(8)	86(5)
C(1)	−1808(15)	−336(11)	793(13)	73(8)
C(2)	−2936(13)	−1063(11)	634(11)	54(7)
C(3)	−3967(12)	−942(10)	−293(12)	57(7)
C(4)	−4987(16)	−1674(13)	−527(14)	77(9)
C(5)	−5009(19)	−2497(14)	238(16)	76(10)
C(6)	−3982(20)	−2584(14)	1182(18)	96(11)
C(7)	−2999(17)	−1887(13)	1393(12)	81(9)
C(8)	−6938(16)	−3292(12)	−907(12)	89(10)
C(9)	−7664(18)	−4286(12)	−818(14)	91(10)
C(10)	−8775(18)	−4518(12)	−1823(14)	84(10)
C(11)	−9540(15)	−5492(12)	−1620(12)	83(9)
C(12)	−10681(16)	−5744(11)	−2574(13)	93(9)
C(13)	−11381(17)	−6715(12)	−2325(14)	87(10)
C(14)	−12551(19)	−6951(13)	−3278(16)	114(12)
C(15)	−13299(17)	−7903(13)	−3066(14)	129(12)
C(16)	2428(14)	2243(11)	2199(12)	64(8)
C(17)	3396(18)	3107(12)	2518(15)	73(9)
C(18)	3459(16)	3987(11)	1854(13)	85(9)
C(19)	4321(16)	4765(11)	2139(13)	91(9)
C(20)	5261(15)	4699(11)	3114(11)	68(8)
C(21)	5269(15)	3846(10)	3852(12)	72(8)
C(22)	4362(18)	3064(11)	3538(16)	84(10)
C(23)	7110(14)	5532(10)	4298(11)	72(8)
C(24)	7786(17)	6581(11)	4264(14)	84(10)
C(25)	9026(17)	6700(11)	5203(14)	83(9)
C(26)	9696(15)	7733(10)	5065(13)	89(9)
C(27)	10976(15)	7924(11)	5890(13)	95(9)
C(28)	11657(15)	8902(11)	5663(13)	90(9)
C(29)	12953(18)	9079(13)	6460(16)	103(12)
C(30)	13639(17)	10062(13)	6229(15)	124(12)

[a] Equivalent isotropic U defined as one third of the trace of the orthogonalised U_{ij} tensor.

We thank the Royal Society, SERC, the University of Sheffield, the British Council and the EC Twinning (Contract No. ST2J—0387C) for support, Johnson Matthey for loans of gold salts and Dr Wim Bras (Daresbury Laboratory) for experimental assistance.

References

1 A-M. Giroud-Godquin and P. M. Maitlis, *Angew. Chem., Int. Edn. Engl.*, 1991, **30**, 375.
2 D. W. Bruce, D. A. Dunmur, P. M. Maitlis, M. R. Manterfield and R. Orr, *J. Mater. Chem.*, 1991, **1**, 255.
3 I. V. Ovchinnikov, Yu. G. Galyametdinov, G. I. Ivanova and L. M. Yagforova, *Dokl. Akad. Nauk. SSSR*, 1984, **276**, 126; S. Chandrasekhar, B. K. Sadashiva, S. Ramesha and B. S. Srikanta, *Pramana J. Phys.*, 1986, **27**, L713; M. Marcos, P. Romero and J. L. Serrano, *J. Chem. Soc., Chem. Commun.*, 1989, 1641.
4 Yu. G. Galyametdinov, G. I. Ivanova and I. V. Ovchinnikov, *Zh. Obshch. Khim.*, 1984, **54**, 2796; Yu. G. Galyametdinov, I. G. Bikchantaev and I. V. Ovchinnikov, *Zh. Obshch. Khim.*, 1988, **58**, 1326; J. L. Serrano, P. Romero, M. Marcos and P. J. Alonso, *J. Chem. Soc., Chem. Commun.*, 1990, 857.
5 C. Bertram, D. W. Bruce, D. A. Dunmur, S. E. Hunt, P. M. Maitlis and M. McCann, *J. Chem. Soc., Chem. Commun.*, 1991, 69.
6 A-M. Giroud, A. Nazzal and U. T. Mueller-Westerhoff, *Mol. Cryst. Liq. Cryst.*, 1980, **56**, 225.
7 K. L. Marshall and S. D. Jacobs, *Mol. Cryst. Liq. Cryst.*, 1988, **159**, 181.
8 H. Adams, N. A. Bailey, D. W. Bruce, R. Dhillon, D. A. Dunmur,

S. E. Hunt, E. Lalinde, A. A. Maggs, R. Orr, P. Styring, M. S. Wragg and P. M. Maitlis, *Polyhedron*, 1988, **7**, 1861.
9 K. Ohta, H. Ema, Y. Morizumi, T. Watanabe, T. Fujimoto and I. Yamamoto, *Liq. Cryst.*, 1990, **8**, 311.
10 R. W. Bost and W. J. Mattox, *J. Am. Chem. Soc.*, 1930, **52**, 332.
11 D. Demus and H. Zaschke, in *Flüssige Kristalle in Tabellen*, VEB Deutscher Verlag für Grundstoffindustrie, Leipzig, 1984, vol. II.
12 C. Furlani and M. L. Luciani, *Inorg. Chem.*, 1968, **7**, 1586.
13 M. Bonamico, G. Dessy and V. Fares, *J. Chem. Soc., Dalton Trans.*, 1977, 2315.
14 O. Piovesana, C. Bellitto, A. Falmini and P. F. Zanazzi, *Inorg. Chem.*, 1979, **18**, 2258; C. Bellitto, A. Flamini, O. Piovesana and P. F. Zanazzi, *Inorg. Chem.*, 1980, **19**, 3632; C. Bellitto, G. Dessy and V. Fares, *Inorg. Chem.*, 1985, **24**, 2815.
15 C. Bellitto, A. Flamini, O. Piovesana and P. F. Zanazzi, *Inorg. Chem.*, 1980, **19**, 3632; C. Bellitto, G. Dessy, V. Fares and A. Flamini, *J. Chem. Soc., Chem. Commun.*, 1981, 409; C. Bellitto, M. Bonamico, G. Dessy, V. Fares and A. Flamini, *J. Chem. Soc., Dalton Trans.*, 1987, 35.
16 M. Bonamico, G. Dessy, V. Fares and L. Scaramuzza, *J. Chem. Soc., Dalton Trans.*, 1972, 2515.
17 See e.g. M. Bonamico, G. Mazzone, A. Vaciago and L. Zambonelli, *Acta Crystallogr.*, 1965, **19**, 898.
18 D. W. Bruce, D. A. Dunmur, S. E. Hunt, P. M. Maitlis and R. Orr, *J. Mater. Chem.*, 1991, **1**, 857.
19 D. W. Bruce, D. A. Dunmur, M. A. Esteruelas, S. E. Hunt, R. Le Lagadec, P. M. Maitlis, J. R. Marsden, E. Sola and J. M. Stacey, *J. Mater. Chem.*, 1991, **1**, 251; J. P. Rourke, F. P. Fanizzi, N. J. S. Salt, D. W. Bruce, D. A. Dunmur and P. M. Maitlis, *J. Chem. Soc., Chem. Commun.*, 1990, 229.
20 J. P. Fackler Jr. and D. Coucouvanis, *J. Am. Chem. Soc.*, 1967, **89**, 1745.
21 D. W. Bruce, R. Dhillon, D. Guillon and P. Maldivi, unpublished.
22 P. Maldivi, D. Guillon, A-M. Giroud-Godquin, J-C. Marchon, H. Abied, H. Dexpert and A. Skoulios, *J. Chim. Phys.*, 1989, **86**, 1651.
23 G. Albertini, A. Guido, G. Mancini, S. Stizza, M. Ghedini and R. Bartolino, *Europhys. Lett.*, 1990, **12**, 629.
24 D. W. Bruce, R. Dhillon, D. A. Dunmur, P. Espinet and P. M. Maitlis, unpublished.
25 J. P. Fackler Jr., J. A. Fetchin and D. C. Fries, *J. Am. Chem. Soc.*, 1972, **94**, 7323; J. P. Fackler Jr., D. Coucouvanis, J. A. Fetchin and W. C. Seidel, *J. Am. Chem. Soc.*, 1968, **90**, 2784.
26 M. Bonamico, G. Dessy, V. Fares and I. Scaramuzza, *J. Chem. Soc., Dalton Trans.*, 1975, 2250.
27 H. Adams, N. A. Bailey, D. W. Bruce, D. A. Dunmur, E. Lalinde, M. Marcos, C. Ridgway, A. J. Smith, P. Styring and P. M. Maitlis, *Liq. Cryst.*, 1987, **2**, 381.
28 M. Bonamico, G. Mazzone, A. Vaciago and L. Zambonelli, *Acta Crystallogr.*, 1965, **19**, 898.
29 H. Iwasaki, *Acta Crystallogr., Sect. B*, 1973, **29**, 2115; H. Iwasaki, M. Ito and K. Kobayashi, *Chem. Lett.*, 1978, 1399.
30 A. Domenicano, L. Torelli, A. Vaciago and L. Zambonelli, *J. Chem. Soc. A.*, 1968, 1351.
31 G. Ungar and J. Feijoo, *Mol. Cryst., Liq. Cryst.*, 1990, **180B**, 281.
32 A. J. Leadbetter, R. M. Richardson and C. N. Colling, *J. Phys.*, 1975, **36**, C1.
33 M. Maltese, *J. Chem. Soc., Dalton Trans.*, 1972, 2664.
34 *International Tables for X-ray Crystallography*, Kynoch Press, Birmingham, 1974, vol. 4.
35 G. M. Sheldrick, *SHELXTL, An integrated system for solving, refining and displaying crystal structures from diffraction data* (Revision 4), University of Göttingen, 1983.

Paper 1/02052H; *Received* 1*st May*, 1991